Theoretical study on the structural, mechanical, electronic properties and QTAIM of CrB_4 as a hard material*

Xiao-Hong Li(李小红)[1,2,†], Hong-Ling Cui(崔红玲)[1], and Rui-Zhou Zhang(张瑞州)[1]

[1] College of Physics and Engineering, Henan University of Science and Technology, Luoyang 471003, China
[2] Department of Chemistry, University of Calgary, Calgary, T2N1N4, Canada

(Received 14 April 2017; revised manuscript received 23 May 2017; published online 18 July 2017)

Using the first-principles calculations based on spin density functional theory (DFT), we investigate the structure, elastic properties, and electronic structure of *Pnnm*-CrB_4. It is found that *Pnnm*-CrB_4 is thermodynamically and mechanically stable. The calculated elastic properties such as the bulk modulus, shear modulus, Young's modulus, and Poisson's ratio indicate that CrB_4 is an incompressible material. Vicker's hardness of *Pnnm*-CrB_4 is estimated to be 26.3 GPa, which is in good agreement with the experimental values. The analysis of the investigated electronic properties shows that *Pnnm*-CrB_4 has the metallic character and there exist strong B–B and Cr–B bonds in the compound, which are further confirmed by Bader's quantum theory of atoms in molecules (QTAIM). Thermodynamic properties are also investigated.

Keywords: first-principles, elastic property, electronic property, QTAIM

PACS: 62.20.Dc, 63.20.dk, 63.20 Dj **DOI:** 10.1088/1674-1056/26/9/096201

1. Introduction

It is an important research to search for the exceptional physical properties in condensed matter physics. Because of their outstanding properties such as high hardness, high electrical conductivity, and better corrosion resistance,[1–3] transitional-metal borides (TMB) represent an exciting case study and have been applied in many applications from creating machining tools to reducing the wear of everyday objects. These materials consist of small, light element B and large, electron-rich transition metals (Cr, Mn, Ru, W, ...). The strong directional covalent bonds between the light element boron and the TM result in the high hardness,[4] and the high density of valence electrons from the transition metals can cause the higher bulk modulus under hydrostatic, both of which can enhance TMB against large plastic deformation and lead to increased hardness.

In recent years, many researchers have successfully synthesized many transitional-metal boron compounds, such as OsB_2,[5] ReB_2,[5] RuB_4,[6] and WB_4.[7] Among these compounds, TM tetraborides (TMB_4) are promising candidates of ultraincompressible and hard materials for their high hardness due to the high content of boron. For example, the hardness of WB_4 is found to be 46.2 GPa because of the three-dimensional boron networks.[6] Many researchers have focused on the tetraborides of transition metals with strong covalent bonds, which can improve the abilities to resist shear deformations.[8] While Os, Re, Ru, and W are all noble metals, which hinder their production and application in industry.

As one of the transition metal tetraborides, chromium tetraboride (CrB_4) was first synthesized in 1968[9] and reported to have excellent adhesive wear resistance because of the outstanding hardness.[10] CrB_4 can also be used as a surface protecting coating because of its good mechanical properties. The single crystal of CrB_4 was first obtained by Knappschneider.[11] Liu *et al.*[12] obtained crystalline, multiphase CrB_4 and showed that CrB_4 crystallizes in the orthorhombic space group *Pnnm*, which is closely related to the space group *Immm* used to describe the orthorhombic structure of CrB_4. Recent researches[13] show that *Immm*-CrB_4 is both dynamically and thermodynamically unstable relative to *Pnnm*-CrB_4.

Recently, Knappschneider *et al.*[14] synthesized *Pnnm*-CrB_4 single crystal, but they did not obtain the elastic moduli of *Pnnm*-CrB_4 from the experiment. They thought that the hardness of *Pnnm*-CrB_4 may be in the range of 43–48 GPa.[14] Wang *et al.*[13] predicted that the bulk modulus of *Pnnm*-CrB_4 is 232 GPa and CrB_4 has a much higher asymptotic hardness of $\sim$ 30 GPa because of the strong three-dimensional Cr–B. The results of Knappschneider *et al.*[14] and Wang *et al.*[13] deviate for the hardness of *Pnnm*-CrB_4. In addition, to the best of our knowledge, the electronic and elastic properties have not been reported for the ground state of CrB_4.

In this paper, the electronic, mechanical properties and Bader charge of *Pnnm*-CrB_4 are investigated by using the first-principles calculations. The hardness of the CrB_4 crystal is estimated theoretically and compared with the two experimental results.[13,14]

*Project supported by the National Natural Science Foundation of China (Grant No. U1304111), Program for Science & Technology Innovation Talents in Universities of Henan Province, China (Grant No. 14HASTIT039), and the Innovation Team of Henan University of Science and Technology, China (Grant No. 2015XTD001).

†Corresponding author. E-mail: lorna639@126.com

© 2017 Chinese Physical Society and IOP Publishing Ltd

2. Methodology

The calculation of structural and electronic properties was performed within the generalized gradient approximation (GGA) by using the plane-wave self-consistent field (PWSCF), which is implemented in the Quantum-Espresso package.[15] The calculations were performed with the spin density functional theory. The exchange–correlation term was treated with Perdew, Burke, and Ernzerhof, known as PBE generalized-gradient approximation.[16] The initial crystal structure was taken from Andersson's result[17] and used for the computations. During the geometric optimization, no symmetry and no restriction were constrained for both the unit cell shape and the atomic positions. A 50 Ry energy cutoff and a 6×6×6 Monkhorst–Pack mesh of k-points were used to ensure the convergence of the total energy within 1 meV per formula unit. To obtain the electronic density of state (DOS), the tetrahedron method with Blochl corrections was used for the Brillouin-zone integration.

Elastic constants were calculated by using the Cambridge serial total energy package (CASTEP) program.[18] The compound was first optimized by using the Broydon–Fletcher–Goldfarb–Shanno (BFGS) method.[19] The ultrasoft pseudopotential[20] together with the generalized gradient approximation (GGA) proposed by Perdew *et al.*[16] was adopted. The bulk modulus B and shear modulus G were obtained from the calculated elastic constants C_{ij}. The Vickers hardenss H_v was also estimated. In addition, the Young's modulus Y and Poisson's ratio ν were predicted.

3. Results and discussion

3.1. Crystal structure of *Pnnm*-CrB_4

CrB_4 is in an orthorhombic system with space group *Pnnm* and its crystal structure[21,22] is shown in Fig. 1. Table 1 lists the lattice constants and structural parameters of *Pnnm*-CrB_4, the experimental values are also included. Obviously, the calculated results are in good agreement with the experimental ones, which confirms the reliability of our computation.

As shown in Fig. 1, each Cr atom is surrounded by twelve B atoms and two Cr atoms. Each B atom is bonded with three Cr atoms and four B atoms. The B_5, B_6, B_7, and B_8 atoms are identical and the distance from these atoms to the Cr_1 atom is 2.050 Å, representing the stronger bonding between Cr and B atoms. While B_1, B_2, B_3, and B_4 atoms are identical and the distance from these atoms to Cr_1 atom is 2.216 Å, indicating the weaker interaction. In addition, B_1, B_2, B_3, B_4, B_5, B_6, B_7, and B_8 atoms form the zigzag boron chains and the B_1–B_4 bond length is about 1.730 Å, which is much shorter than the B–B bond length of the binary borides such as WB (B–B 1.891 Å[23]) and CrB (B–B 1.780 Å[24]), but slightly longer than the B–B bond length (1.721 Å[24]) of CrB_2. The shorter bond length may play an important role in resisting the plastic deformation. The computed lattice constants are also close to those determined experimentally.

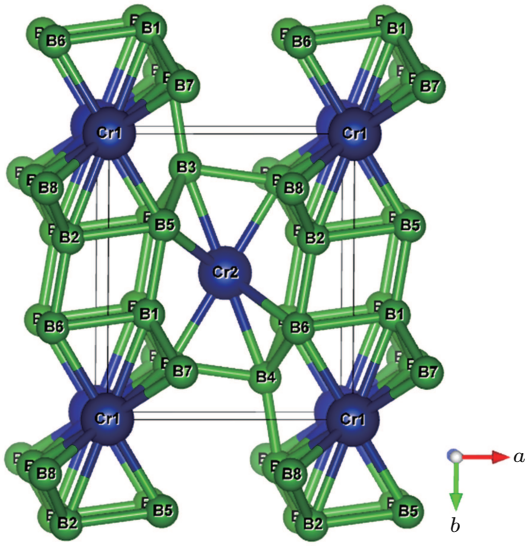


Fig. 1. (color online) Crystal structures and its atomic numbering of *Pnnm*-CrB_4. The blue and green spheres represent Cr and B atoms, respectively.

Table 1. Experimental and calculated lattice constants and bond lengths (Å) of *Pnnm*-CrB_4 crystal at ambient pressure.

Lattice constants			
$a = 4.766(4.7482)^*$ $b = 5.507(5.4856)$ $c = 2.857(2.8717)$			
volume =74.986(74.798)			
Bond length/Å		Bond angle/(°)	
Cr_2–B_1	2.216(2.219)	B_1–Cr_2–B_4	45.8.(45.387)
Cr_2–B_6	2.050(2.099)	B_4–Cr_2–B_7	50.2(50.637)
Cr_2–B_4	2.216(2.217)	B_6–Cr_2–B_8	52.1(51.862)
Cr_2–B_7	2.050(2.099)	B_8–Cr_1–B_3	50.2(50.637)
B_6–B_8	1.852(1.836)	B_8–B_6–B_1–Cr_2	51.8(51.963)
B_6–B_1	1.837(1.849)	B_6–B_1–Cr_2–B_4	156.4(156.603)
B_1–B_4	1.730(1.710)	Cr_2–B_3–B_8–Cr_1	–180.0(–180.0)
B_4–B_7	1.839(1.849)	Cr_1–B_8–Cr_2	129.7(129.363)
Cr_1–Cr_2	3.918(3.901)	Cr_1–B_3–Cr_2	129.7(129.363)

*The values in parentheses are experimental values taken from Ref. [16].

3.2. Elastic properties

Further calculations were performed to optimize the lattice constants within a given energy cutoff of 50 Ry. The total energy versus the volume is plotted in Fig. 2. Fitting the data of the total energy and the volume to the Birch–Murnaghan equation of state,[25] we can obtain the bulk modulus B and the equilibrium volume V, which can be compared with the results obtained by the CASTEP calculation. The obtained bulk modulus B and equilibrium volume from the Birch–Murnaghan equation of state are 278.25 GPa and 75.48 $Å^3$, respectively. The pressure derivative of the bulk modulus is 4.53. The obtained bulk modulus is much smaller than that of diamond (442 GPa).[26]

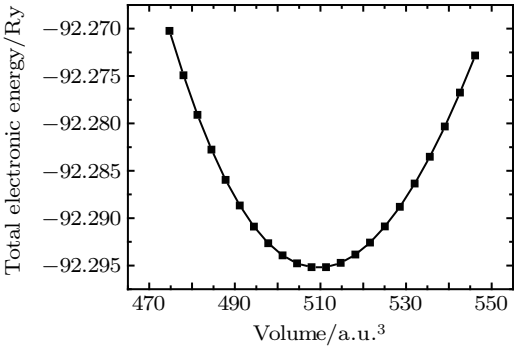


Fig. 2. The total energy versus volume.

Obviously, the equilibrium volume is much closer to the calculated value 74.987 Å^3 and the experimental value 74.798 Å^3, which shows that our calculation is reliable. Table 2 lists the calculated elastic constants C_{ij} (GPa), bulk moduli B (GPa), shear moduli G (GPa), Young's moduli E (GPa), the G/B ratio, Poisson's ratio ν, and Vicker's hardness $H_{\rm v}$ (GPa) at ambient pressure. The available experimental and calculated values are also included. In order to have a comparison, the experimental and calculated hardnesses of diamond and B_4C are also listed in Table 2.

Table 2. Calculated elastic constants C_{ij} (GPa), bulk moduli B (GPa), shear moduli G (GPa), Young's moduli E (GPa), the G/B ratio, Poisson's ratio ν, and Vicker's hardness $H_{\rm v}$ (GPa) at ambient pressure, compared with available experimental and theoretical results. The values in parentheses are experimental values and the others are computational values.

C_{11}	C_{22}	C_{33}	C_{44}	C_{55}	C_{66}	C_{12}	C_{13}	C_{23}	B	G
582, 542[a]	936, 927[a]	481, 488[a]	254, 254[a]	279, 281[a]	220, 257[a]	60, 73[a]	112, 94[a]	91, 97[a]	273, 263[a]	260, 267[a]
E	G/B	ν	$H_{\rm v}$	$H_{\rm v}^{\rm Equ(2)}$	$H_{\rm v}^{\rm Equ(3)}$	$H_{\rm v}^{\rm Equ(4)}$	$H_{\rm v}^{\rm Equ(5)}$	$H_{\rm v4}^{\rm BC}$	$H_{\rm v}^{\rm c-BN}$	$H_{\rm v}^{\rm Diamond}$
592, 599[a]	0.95	0.14, 0.12[a]	23–26[b]	45.9	43.1	26.3	35.4	31.7[b]	65.2[b] (66)[b]	95.7[b] (96)[b]

[a]Data taken from Ref. [27]; [b]the value is taken from Ref. [13].

For the orthorhombic system, 9 independent components of the elastic constants must satisfy the following necessary conditions for mechanical stability:[28]

$$\begin{aligned} &C_{11}+C_{22}+C_{33}+2C_{12}+2C_{13}+2C_{23}>0,\\ &C_{22}+C_{33}-2C_{23}>0,\\ &C_{ii}>0, \quad (i=1,2,\ldots,6). \end{aligned} \tag{1}$$

From Table 2, the whole set of elastic constants C_{ij} satisfy the mechanical stability criteria,[28] implying the mechanical stability of the studied structure at ambient pressure. The calculated bulk modulus is 273 GPa, which is close to the fitted value (278 GPa) from the Birch–Murnaghan equation of state. This indicates that CrB_4 can be grouped into incompressible materials. The shear modulus and Pugh's ratio[29] ($K=G/B$) are two important elastic properties which are thought to be related with the hardness based on the empirical formulation of Chen *et al.*[30] For polycrystalline materials, the hardness can be written as

$$H_{\rm v}=2(K^2G)^{0.585}-3, \tag{2}$$

where $K=G/B$.

In order to have a comparison, the other methods to calculate the hardness of bulk material are also used to calculate the hardness of CrB_4. One is Teter's model[31]

$$H_{\rm v}=0.1769G-2.899. \tag{3}$$

The others are obtained by Jiang *et al.*[32]

$$H_{\rm v}=0.0963B, \tag{4}$$

$$H_{\rm v}=0.0607E. \tag{5}$$

Using Eqs. (2)–(5), the hardness of *Pnnm*-CrB_4 is estimated to be 45.9 GPa, 43.1 GPa, 26.3 GPa, and 35.4 GPa, respectively. The hardness obtained using Eq. (4) is in good agreement with the experimental values of 23–26 GPa[13] because the bulk modulus measures the resistance of a crystal to volume change. In addition, the theoretically estimated values of 43–48 GPa also reflect the general difficulty to estimate hardness from first-principles calculations.[12] It is noted that the hardness of *Pnnm*-CrB_4 is much larger than that of B_4C, but smaller than that of c-BN and diamond.

For CrB_4, the shear modulus G is 260 GPa, which shows that *Pnnm*-CrB_4 has the strong ability to resist shear change. The low Poisson ratio for *Pnnm*-CrB_4 shows that strong covalent bonding exists in CrB_4.[33] Pugh's ratio of CrB_4 is 0.95. The G/B value is often used to assess the brittle or ductile behavior of a compound. Low G/B denotes better ductility, and a critical value of G/B is 0.57.[26] The larger the G/B value, the higher the Vickers hardness. Obviously, the G/B value for *Pnnm*-CrB_4 is much larger than the critical value, so CrB_4 can be classified as a brittle material.

In addition, B_a, B_b, and B_c (the bulk moduli along a-, b-, and c-axes) are also calculated according to the method of Nye[34] and their values are 756 GPa, 1209 GPa, and 620 GPa, respectively, which are much larger than those of YB_4 (571 GPa, 571 GPa, and 499 GPa).[35] It is noted that the b-axis is less compressible than a- and c-axes because the zigzag boron–boron chains are primarily along the direction. For a- and c-directions, the strengths of the Cr–B and Cr–Cr bonds determine the axial compressibility. In addition, C_{22} of *Pnnm*-CrB_4 is 936 GPa, which is much larger than the largest component C_{11} (794 GPa)[36] of d-ZB-C_3N_4. This indicates

that *Pnnm*-CrB_4 may be highly incompressible along the *b*-axis, which is consistent with the conclusion obtained from the bulk moduli.

In order to check the dynamical stability of *Pnnm*-CrB_4, the phonon dispersion curve is calculated and plotted in Fig. 3. A stable crystalline structure requires phonon frequencies to be positive, so no imaginary phonon frequencies in the whole Brillouin zone in Fig. 3 confirm the dynamical stability of *Pnnm*-CrB_4 at ambient pressure.

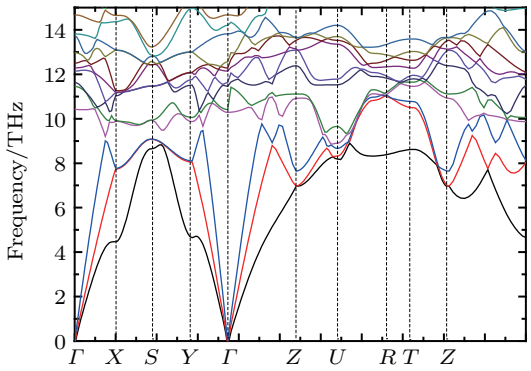


Fig. 3. (color online) The phonon-dispersion curve of *Pnnm*-CrB_4.

3.3. Electronic structure

The electronic band structure of *Pnnm*-CrB_4 has been studied along the high-symmetry points of the Brillouin zone and plotted in Fig. 4(a). Fermi energy levels are all indicated in Fig. 4. From Fig. 4(a), the overlap between the conduction band (CB) and the valence band (VB) indicates that *Pnnm*-CrB_4 has a metallic character. In order to further understand the element contribution to the electronic structure of *Pnnm*-CrB_4, the total and projected density of states (PDOS) for *Pnnm*-CrB_4, Cr, and B are plotted in Figs. 4(b) and 4(c), respectively. From Fig. 4(b), it is noted that *Pnnm*-CrB_4 exhibits metallic behavior because of the finite electronic DOS at the Fermi level.

From Figs. 4(b) and 4(c), the low VB is mainly dominated by 3d states of Cr atoms and 2p states of B atoms below the Fermi level (the Fermi level is shifted to zero). The 2s states of B atoms also contribute to the VB, although the densities of states are quite small compared to those of the 3d states of Cr atoms. The 3d states of Cr atoms and 2p states of B atoms contribute to the CB of *Pnnm*-CrB_4 and dominate the DOS at the Fermi level, which indicates strong interaction and hybridization between the orbitals of Cr 3d and B 2p. In addition, it is noted that the partial DOS profiles for Cr 3d states and B 2p states are very similar from −10 eV to 3 eV and overlap each other, which shows the strong hybridization between the orbitals of Cr 3d and B 2p and further confirms the strong covalent Cr–B bond. From Figs. 4(b) and 4(c), there is a deep valley at the Fermi level, which is a pseudogap of DOS and considered as the borderline between the bonding and antibonding states.[37] The pseudogap at the Fermi level also shows that the bonding between Cr 3d and B 2p starts to be saturated.

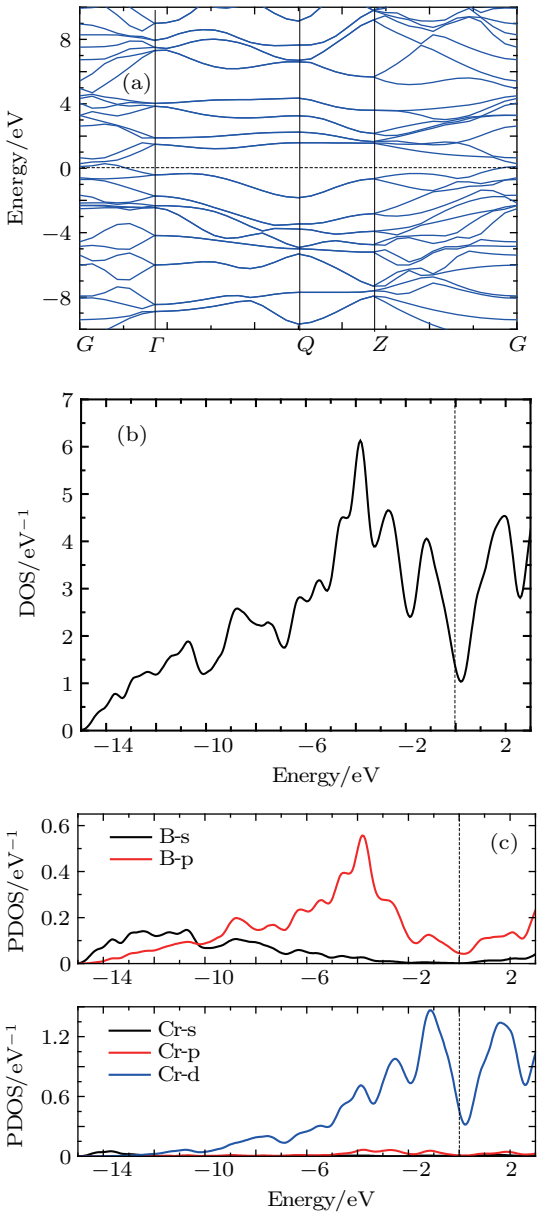
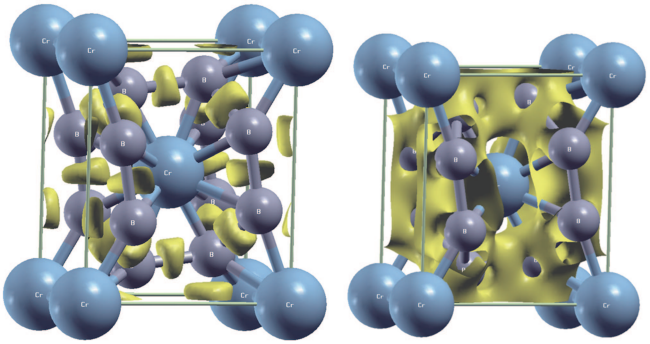


Fig. 4. (color online) (a) The band structure of *Pnnm*-CrB_4 along the high-symmetry points. (b) The total density of state of *Pnnm*-CrB_4. (c) The partial density of states of Cr and B atoms. The Fermi level is at the energy 0 eV.

In order to explore the bonding character of *Pnnm*-CrB_4, the electron localization function (ELF) is calculated. The ELF can be used to measure the probability of finding an electron in the neighborhood of another electron with the same spin. The ELF ranges from 0 to 1. ELF = 1 means perfect localization (i.e. a covalent bond), ELF = 0.5 corresponds to the electron-gas like pair probability (i.e., a metallic bond), while ELF = 0 corresponds to no localization (or delocalized electrons). Figure 5 shows the calculated ELF of *Pnnm*-CrB_4 with isosurfaces at ELF equaling to 0.5 and 0.8, respectively.

In Fig. 5(a), the ELF between two adjacent B and B

atoms is nearly 1, indicating the strong B–B covalent bond. In Fig. 5(b), the ELF at the Cr sites is negligible and the ELF at the B sites attains the local maximum, which indicates partially covalent Cr–B bonds. In addition, from Fig. 5, we can see that the overall ELF at the B sites is higher than that at the Cr sites. In addition, the strong B–B bonds between the neighbor boron atoms may increase the structural stabilities and high bulk moduli of *Pnnm*-CrB_4.



(a) ELF = 0.8 (b) ELF = 0.5

Fig. 5. (color online) The electron localization functions of three-dimensional framework for *Pnnm*-CrB_4 with ELF equaling to 0.8 and 0.5, respectively. The large and small spheres represent the Cr and B atoms, respectively.

3.4. Quantum theory of atoms in molecules

Table 3 lists the calculated partial charges of *Pnnm*-CrB_4. From Table 3, it is noted that the Cr atoms donate electrons, while the B atoms accept electrons. The charge on B_1, B_2, B_3, and B_4 atoms is nearly the same and smaller than that on B_5, B_6, B_7, and B_8 atoms. The reason may be that the distances of B_5, B_6, B_7, and B_8 from Cr_1 and Cr_2 are 2.050 Å and 2.167 Å, respectively, which are smaller than those of B_1, B_2, B_3, and B_4 atoms from Cr_1 and Cr_2 (2.216 Å and 2.539 Å, respectively). So B_5, B_6, B_7, and B_8 atoms accept more electrons from Cr_1 and Cr_2 atoms.

Table 3. Partial charge (e) of the Cr and B atoms in *Pnnm*-CrB_4.

Atom	Charge	Atom	Charge
Cr_1	0.8316473	B_4	–0.078286
Cr_2	0.8316473	B_5	–0.3353168
B_1	–0.078286	B_6	–0.3352273
B_2	–0.0828364	B_7	–0.3352273
B_3	–0.0828178	B_8	–0.3352981

Based on the topology of the electronic density, Bader's quantum theory of atoms in molecules (QTAIM) is a useful tool to explain physical and chemical properties of materials. QTAIM analysis[38,39] starts by determining the critical points (CPs) of the electron density, which are classified into maxima, nuclear, or attractor CPs (NCP or n); first-order saddle or bond (BCP or b); second-order saddle or ring (RCP or r); and minima or cage (CP or c). For a predominantly "shared" (covalent) interaction, $\rho(r) > 0$ and $\nabla^2\rho < 0$.[33] In the case of a "closed shell" (ionic) interaction, ρ(r) is usually small ($\sim 10^{-2}$ a.u. for an H-bond and $\sim 10^{-3}$ a.u. for a van der Waals' interaction[39]) whilst $\nabla^2\rho > 0$. The sign and magnitude of the total energy density component[40] at a BCP, H(r), are also important parameters of the nature of the bonding[41,42] and can be obtained by the following equation:

$$H(r) = G(r) + V(r), \tag{6}$$

$$\xi = \frac{|V(r)|}{G(r)}, \quad \text{if} \begin{cases} \xi < 1, & \text{ionic bond type,} \\ \xi > 2, & \text{covalent bond type,} \\ 1 < \xi < 2, & \text{intermediate bond type,} \end{cases} \tag{7}$$

where $V(r)$ is the local electron potential energy density, and $G(r)$ is the local electron kinetic energy density. For a covalent interaction, $V(r)$ dominates and $H(r) < 0$, while $G(r)$ dominates and $H(r) > 0$ for a predominantly ionic interaction.[43] The ratio ξ is another useful parameter[44] to predict the nature or the characteristic of the chemical atomic interactions.

Table 4. The crystallographic position and properties of CrB_4 electron density bond critical points.

type	Bond	Position (cr ystal coord.)	$\rho(r_c)$ /e·Å^{-3}	$\nabla^2\rho(r_c)$ /e·Å^{-5}	$H(r_c)$ /Hartree·Å^{-3}	$G(r_c)$ /Hartree·Å^{-3}	$V(r_c)$ /Hartree·Å^{-3}	ξ	λ_1 /e·Å^{-5}	λ_2 /e·Å^{-5}	λ_3 /e·Å^{-5}	d_1/Å[b]	d_2/Å[b]	D/Å[c]
b1	B–B	(0.7607 0.5457 0.0017)	0.1211	–0.2042	–0.1362	0.0852	–0.2214	2.5986	–39.07	–0.25	39.12	0.1533	0.0484	0.2017
b2	B–B	(0.0969 0.3021 0.0017)	0.1131	–0.3494	–0.1633	0.0759	–0.2392	3.1515	–23.73	–0.16	23.54	0.0479	0.0656	0.1135
b3	B–B	(0.6064 0.6381 0.2337)	0.1188	–0.1206	–0.0368	0.0294	–0.0662	2.2517	–1.40	–0.01	1.38	0.0556	2.0158	2.0714
b4	Cr–B	(0.5520 0.3217 0.4983)	0.0746	0.2623	–0.0226	0.0380	–0.0604	1.5895	–3.08	–0.04	3.38	0.0698	0.0581	0.1279
b5	Cr–B	(0.5605 0.6713 0.4967)	0.0644	0.2163	–0.0233	0.0297	–0.053	1.7854	–2.84	–0.02	3.07	0.0713	0.0641	0.1354

[a] λ_1, λ_2, λ_3: eigenvalues; [b] d_1, d_2: the distance between bcp and each bonded atom; [c] D: total bond path length.

It is noted from Table 4 that high electron densities compared with the other bonds for b1, b2, and b3 and the negative Laplacian values indicate that b1, b2, and b3 have the significant covalent character. Specially, using the ratio ξ as a diagnostic, $\xi > 2$ further confirms the covalent nature of b1, b2, and b3. For the b4 and b5 bonds, $1 < \xi < 2$ indicates that the Cr–B bonds have intermediate character, which is consistent with the analysis of ELF. The three curvatures (λ_1, λ_2, and λ_3) of electronic density ρ, the distances between BCP and each bonded atom, and the total bond path length are also included in Table 4.

Through the quasi-harmonic Debye model, the thermodynamic quantities are calculated for CrB_4 from the calculated E–V data at $T = 0$ and $P = 0$. Figure 6 displays the heat capacities (C_v), free energy (F), and entropy (S) versus temperature up to $T = 2000$ K at zero pressure for CrB_4. It is observed that C_v increases sharply with the increasing temperature for $0 < T < 300$ K and approaches the Dulong–Petit classical limit at high temperatures. This indicates that the optical and acoustic modes are all excited at the temperature. It is known that the free energy of a structure is closely related to its geometrical structure. From Fig. 6, the free energy decreases gradually with the increase of the temperature, while the entropy increases when the temperature increases. This behavior is understandable because the phonon frequency should increase with temperature. The heat capacities (C_v) and entropy (S) are zero at 0 K, which is in complete agreement with the third law of thermodynamics.

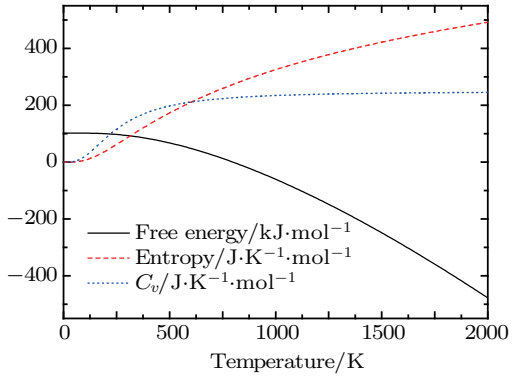


Fig. 6. (color online) Variation with the temperature of the heat capacity, entropy and free energy of CrB_4.

4. Conclusion

We performed an extensive exploration of the *Pnnm*-CrB_4 crystal in the ground state by using spin density functional theory. Through the analysis of elastic constants and the phonon frequencies, *Pnnm*-CrB_4 is found to be thermodynamically and mechanically stable. The high bulk moduli of *Pnnm*-CrB_4 indicate that *Pnnm*-CrB_4 is an incompressible material. The analysis of the elastic constants indicates that *Pnnm*-CrB_4 may be highly incompressible along the *b*-axis. The electronic densities of states and electronic localization function analysis have demonstrated that there exist the strong covalent B–B bonding and Cr–B bonds with an intermediate character in the *Pnnm*-CrB_4 crystal. At the Fermi level, there exists a pseudogap of DOS which mainly comes from Cr 3d states and B 2p states. The pseudogap at the Fermi level shows that the bonding between Cr 3d and B 2p starts to be saturated. The analysis of Bader charge indicates that B_5, B_6, B_7, and B_8 atoms accept more electrons from Cr_1 and Cr_2 atoms, when compared with B_1, B_2, B_3, and B_4 atoms. The analysis of Bader's quantum theory of atoms in molecules further confirms the intermediate character of Cr–B bonds. We believe that the current study will advance the understanding of the properties of *Pnnm*-CrB_4 crystal.

References

[1] Veprek S, Zhang R F and Argon A S 2011 *J. Superhard Mater.* **33** 409
[2] Bao K, Ma S L, Xu C H and Cui T 2017 *Acta Phys. Sin.* **66** 36104 (in Chinese)
[3] Fahrenholtz W G, Hilmas G E, Talmy I G and Zaykoski J A 2007 *J. Am. Ceram. Soc.* **90** 1347
[4] Levine J B, Tolbert S H and Kaner R B 2009 *Adv. Funct. Mater.* **19** 3519
[5] Kaner R B, Gilman J J and Tolbert S H 2005 *Science* **308** 1268
[6] Gu Q, Krauss G and Steurer W 2008 *Adv. Mater.* **20** 3620
[7] Xie M, Mohammadi R, Mao Z, Armentrout M M, Kavner A, Kaner R B and Tolbert S H 2012 *Phys. Rev. B* **85** 064118
[8] Zhang M, Lu M and Du Y 2014 *J. Phys. Chem.* **140** 174505
[9] Andersso S and Lundstro T 1968 *Acta Chem. Scand.* **22** 3103
[10] Sue J A, Tucker R C and Nemeth J P (U.S. Patent) 6 007 922 [1999-04-15]
[11] Knappschneider A, Litterscheid C, Kurzman J, Seshadri R and Albert B 2011 *Inorg. Chem.* **50** 10540
[12] Niu H, Wang J, Chen X Q, Li D, Li Y, Lazar P, Podloucky R and Kolmogorov A N 2012 *Phys. Rev. B* **85** 144116
[13] Wang S, Yu X, Zhang J, Wang L, Leinenweber K, Xu H, Popov D, Park C, Yang W, He D and Zhao Y 2014 *J. Superhard Mater.* **36** 279
[14] Knappschneider A, Litterscheid C, Dzivenko D, Kurzman J A, Seshadri R, Wagner N, Beck J, Riedel R and Albert B 2013 *Inorg. Chem.* **52** 540
[15] Baroni S, Corso A dal, Gironcoli S de, Giannozzi P, Cavazzoni C, Ballabio G, Scandolo S, Chiarotti G, Focher P, Pasquarello A, Laasonen K, Trave A, Car R, Marzari N and Kokalj A <http://www.pwscf.org>
[16] Perdew J P, Nurke K and Ernzerhof M 1996 *Phys. Rev. Lett.* **77** 3865
[17] Andersson S and Lundstroem T 1955 *Acta Chemica Scandinavica* **9** 1107
[18] Segall M D, Lindan P J D, Probert M J, Pickard C J, Hasnip P J, Clark S J and Payne M C 2002 *J. Phys.: Condens. Matter.* **14** 2717
[19] Pfrommer B G, Cote M, Louie S G and Cohen M L 1997 *J. Comput. Phys.* **131** 233
[20] Vanderbilt D 1990 *Phys. Rev. B* **41** 7892
[21] Albert B and Hillebrecht H 2009 *Angew. Chem.* **12** 8794
[22] Albert B and Hillebrecht H 2009 *Angew. Chem. Int. Ed.* **48** 8640
[23] Gou H, Li Z, Zhang J, Gao F, Rodney C and Lian J 2012 *Comput. Mater. Sci.* **53** 460
[24] Ade M and Hillebrecht H 2015 *Inorg. Chem.* **54** 6122
[25] Murnaghan F D 1944 *Proc. Natl. Acad. Sci. USA* **30** 244
[26] Winey J M and Gupta Y M 2013 *Phys. Rev. B* **87** 174104
[27] Xu C, Li Q, Liu C M, Duan M Y and Wang H K 2016 *Inter. J. Modern Phys. B* **30** 1650098
[28] Patil S K R, Khare S V, Tuttle B R, Bording J K and Kodambaka S 2006 *Phys. Rev. B* **73** 104118
[29] Pugh S F 1954 *Philos. Mag. Ser.* **45** 823

[30] Chen X Q, Niu H Y, Li D Z and Li Y Y 2011 *Intermetallics* **19** 1275
[31] Li H, Zhang J and Gou H 2014 *J. Solid State Chem.* **213** 52
[32] Jiang X, Zhao J and Jiang X 2011 *Comput. Mater. Sci.* **50** 2287
[33] Levine J B, Tolbert S H and Kaner R B 2009 *Adv. Funct. Matter.* **19** 3519
[34] Nye J F 1985 *Physical Properties of Crystals* (Oxford: Clarendon Press) pp. 78, 79
[35] Fu Y Y, Li Y W and Huang H M 2014 *Chin. Phys. Lett.* **31** 116201
[36] Tang X, Hao J and Li Y 2015 *Phys. Chem. Chem. Phys.* **17** 27821
[37] Vajeeston P, Ravindran P and Ravi C 2001 *Phys. Rev. B* **63** 045115
[38] Tang W, Sanville E and Henkelman G 2009 *J. Phys.: Condens. Matter.* **21** 084204
[39] Bader R F W and Essén H 1984 *J. Chem. Phys.* **80** 1943
[40] Varadwaj P R and Marques H M 2010 *Phys. Chem. Chem. Phys.* **12** 2126
[41] Cramer D and Kraka E 1984 *Angew. Chem. Int. Ed. Engl.* **23** 627
[42] Cramer D and Kraka E 1984 *Croat. Chem. Acta* **57** 1259
[43] Espinosa E, Alkorta I, Elguero J and Molins E 2002 *J. Chem. Phys.* **117** 5529
[44] Jenkins S and Morrison I 2000 *Chem. Phys. Lett.* **317** 97